

Reactions of the simple nitroalkanes with hydroxide ion in water. Evidence for a complex mechanism†

Zhao Li,^{a,b} Jin-Pei Cheng^{*b} and Vernon D. Parker^{*a}

Received 18th February 2011, Accepted 28th March 2011

DOI: 10.1039/c1ob05270e

Conventional kinetic analysis of the reactions of nitromethane (NM), nitroethane (NE) and 2-nitropropane (2-NP) with hydroxide ion in water revealed that the reactions are complex and involve kinetically significant intermediates. Kinetic experiments at the isosbestic points where changes in reactant and product absorbance cancel indicate the evolution and decay of absorbance characteristic of the formation of reactive intermediates. The deviations from 1st-order kinetics were observed to increase with increasing extent of reaction and in the reactant order: NM < NE < 2-NP. The apparent deuterium kinetic isotope effects for proton/deuteron transfer approach unity near zero time and increased with time toward plateau values as the reaction kinetics reach steady state. It is proposed that the initially formed preassociation complexes are transformed to more intimate reactant complexes which can give products by two possible pathways.

Introduction

The observation¹ of the unusual inverse order of kinetic and thermodynamic acidities of the simple nitroalkanes (nitromethane = NM, nitroethane = NE and 2-nitropropane = 2-NP) during their reactions with hydroxide ion in water more than a half-century ago was later referred to as the nitroalkane anomaly.² Data for this novel relationship are reproduced in Table 1. This phenomenon has perplexed physical organic chemists ever since its discovery and a number of papers were published on the topic for reactions in protic solvents,³ aprotic solvents,⁴ and mixed solvents.⁵

The reactions of aryl nitroalkanes in the presence of benzoic acid buffers in DMSO were observed to be free of complications from ion pairing and a 1-step proton transfer equilibrium was proposed.⁴ A recent study⁶ led to the conclusion: "Calculations also show that the 'nitroalkane anomaly', well established in solution, does not exist in the gas phase." It is important to note at the outset that explanations of the nitroalkane anomaly have generally involved a single transition state on the reaction coordinate, *i.e.* the proton transfers have been assumed to take place in a single step, sometimes followed by rapid hydrogen bonding or ion pairing. An exception to the latter⁷ was the proposal of slow reaction of a hydrogen bonded substrate molecule to an anionic intermediate in which the charge is localized on the

Table 1 Equilibrium and rate data often cited in support of the "nitroalkane anomaly"

Substrate	NM	NE	2-NP
pK _a in water	10.22 ^a	8.60 ^a	7.74 ^b
Relative <i>k</i> _{app} ^c	1.00	0.188	0.0114

^a Ref. 1e. ^b Ref. 1b,c. ^c Ref. 3a corrected for symmetry factor (NM = 3, NE = 2, 2-NP = 1).

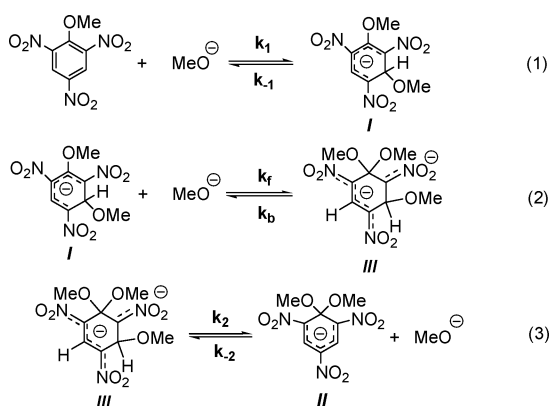
carbon attached to the nitro group by the hydrogen bond. It was later pointed out⁸ that hydrogen bonding to oxygen of the nitronate product by the conjugate acid of the base is more likely than the formation of an intermediate. Reference to a ¹⁴C kinetic isotope effect study⁹ was cited as evidence against the proposed reaction intermediate. We now report convincing experimental evidence that the assumption that rate determining proton transfer is the first step in the mechanism is not correct.

The present work is a part of our general effort to determine the mechanisms of fundamental organic reactions. We have recently shown¹⁰ that the reaction of 2,4,6-trinitroanisole (TNA) with methoxide ion in methanol takes place by a reversible consecutive mechanism (Scheme 1). The latter is contrary to the long-accepted belief that formation of the 2,4,6-trinitro-1,3-dimethoxy-cyclohexadienylide (I) and the 1,1-dimethoxy complex (II) take place by a competitive rather than a sequential mechanism. The tentatively proposed intermediate (III) was not observed but the ¹H NMR spectrum had previously been recorded.¹¹ A reversible consecutive mechanism was previously proposed for the proton transfer reaction between 1-nitro-1-(4'-nitrophenyl)ethane (NNPE) with hydroxide ion in aqueous acetonitrile.¹²

^aDepartment of Chemistry and Biochemistry, Utah State University, Logan, UT, 84322, USA. E-mail: vernon.parker@usu.edu

^bDepartment of Chemistry, The State Key Laboratory of Elemento-Organic Chemistry, Nankai University, Tianjin, 300071, China

† Electronic supplementary information (ESI) available: Details of the kinetic data and profiles under various conditions. See DOI: 10.1039/c1ob05270e

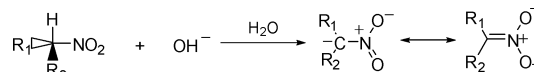


Scheme 1 Proposed mechanism for the reaction of TNA with methoxide ion in methanol.

Results and discussion

Absorbance–time profiles for the evolution of products at 240 nm over several half-lives for the reactions of NM, NE and 2-NP with hydroxide ion in water at 298 K are illustrated by the plots in the left column of Fig. 1. (Spectra of anions of nitroalkanes in water have been reported.¹³ Reactant spectra and extinction coefficients of NM, NE and 2-NP are shown in Fig. S4, electronic supplementary information (ESI)).[†] It is evident that the reactions go to completion and the absorbance values at the plateaus indicate that the reaction products are stable during the time periods of the experiments. ¹H NMR spectra of reaction mixtures after several half-lives show no significant signals indicative of side-products. The acid–base reactions produce the conjugate bases

according to Scheme 2 where the anionic products are represented as two resonance forms showing the distribution of the negative charge.



Scheme 2 Reactions of nitroalkanes with hydroxide ion in water.

The conventional first-order analyses of the reactions are revealing in terms of whether or not the reactions conform to first-order kinetics as is expected from the previous studies.³ The latter is illustrated by the $\ln(1 - \text{E.R.})$ –time profiles, where E.R. is the extent of reaction, along with the corresponding least squares correlation lines. The degrees of deviation of the experimental data from the correlation lines were observed to be inversely related to the kinetic reactivity of the nitroalkane, *i.e.* deviations are more pronounced in the order, 2-NP > NE > NM. The latter was also observed to increase with increasing E.R. and the data for 2-NP began to deviate from that expected for first-order kinetics during the first half-life of the reaction while deviations for the other two substrates became significant at greater E.R. The relationships are illustrated by the plots in the right column of Fig. 1 and in more detail in the ESI.[†]

In order to be able to describe the deviations of the nitroalkane proton transfer reactions with hydroxide ion in more detail, the least square correlations of $\ln(1 - \text{E.R.})$ –time profiles were carried out incrementally¹⁴ over the 2000 point profiles by two different procedures. In the first, the analyses were carried out on 101 point increments, beginning with data points 1 to 101, followed by data points 101 to 201 and subsequent increments with the final one being from data points 1701 to 1801. The data, summarized in Table 2, clearly show that the apparent first-order rate constants are E.R. dependent, decreasing continuously as the reactions proceed toward completion.

The data in Table 3 were obtained using a modification of the pseudo first-order analysis procedure. The experimental procedure

Table 2 Variations of the apparent pseudo first-order rate constants for the reactions of nitroalkanes with hydroxide ion in water over several half-lives (5 half-lives for NM, 4 half-lives for NE, 3 half-lives for 2-NP)

Point range ^a	k/s^{-1} (NM) ^b	k/s^{-1} (NE) ^b	k/s^{-1} (2-NP) ^c
1–101	0.493	0.240	0.01506
101–201	0.494	0.242	0.01447
201–301	0.492	0.240	0.01377
301–401	0.486	0.234	0.01299
401–501	0.477	0.224	0.01215
501–601	0.465	0.211	0.01131
601–701	0.452	0.195	0.01049
701–801	0.440	0.179	0.00970
801–901	0.430	0.164	0.00896
901–1001	0.423	0.152	0.00824
1001–1101	0.416	0.141	0.00752
1101–1201	0.408	0.129	0.00677
1201–1301	0.394	0.112	0.00597
1301–1401	0.366	0.0885	0.00512
1401–1501	0.322	0.0585	0.00425
1501–1601	0.266	0.0289	0.00344
1601–1701	0.220	0.0117	0.00283
1701–1801	0.221	0.0215	0.00261

^a Described in the text. [NaOH] = ^b 20 mM and ^c 50 mM in H₂O at 298 K.

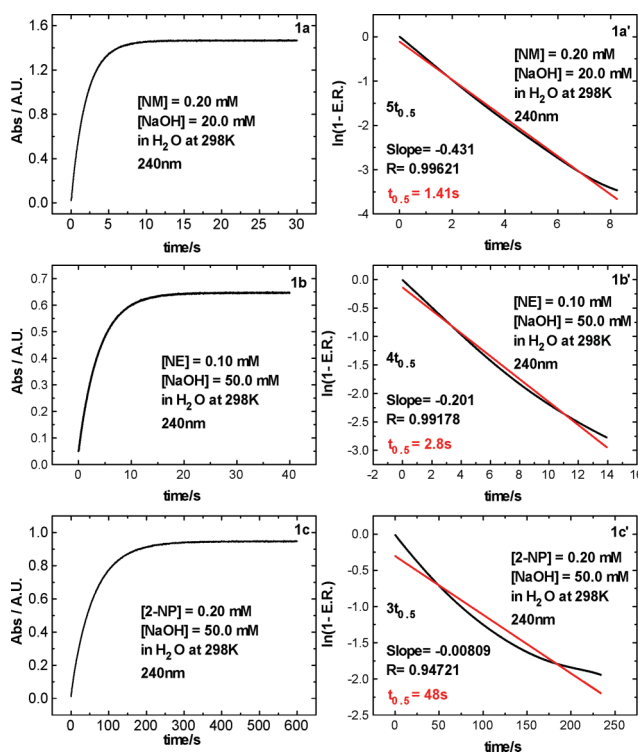


Fig. 1 Absorbance–time profiles (a, b, c) and $\ln(1 - \text{E.R.})$ –time profiles (a', b', c') for the reactions of nitroalkanes (a,a' NM, b,b' NE, c,c' 2-NP) with hydroxide ion in water at 298 K.

Table 3 Apparent rate constants for the reactions of nitroalkanes with hydroxide ion in water over the first half-life at 298 K

NM ^a		NE ^b		2-NP ^c		Segment
k_{app}/s^{-1}	\pm	k_{app}/s^{-1}	\pm	k_{app}/s^{-1}	\pm	
0.478	0.056	0.280	0.010	0.0248	0.0013	1
0.560	0.010	0.276	0.005	0.0223	0.0007	2
0.548	0.002	0.273	0.004	0.0214	0.0005	3
0.545	0.002	0.271	0.002	0.0210	0.0008	4
0.544	0.001	0.269	0.001	0.0206	0.0008	5
0.538	0.003	0.265	0.001	0.0200	0.0008	6
0.531	0.004	0.261	0.001	0.0193	0.0007	7
0.527	0.004	0.259	0.001	0.0187	0.0006	8
0.525	0.004	0.258	0.001	0.0183	0.0006	9
0.523	0.004	0.257	0.001	0.0179	0.0006	10
0.522	0.004	0.256	0.001	0.0176	0.0006	11
0.521	0.005	0.256	0.002	0.0173	0.0006	12
0.519	0.005	0.255	0.002	0.0171	0.0006	13
0.519	0.005	0.255	0.002	0.0170	0.0006	14
0.518	0.005	0.254	0.002	0.0168	0.0006	15
0.517	0.005	0.254	0.002	0.0167	0.0006	16
0.516	0.005	0.253	0.002	0.0166	0.0006	17
0.515	0.005	0.253	0.002	0.0165	0.0006	18
0.514	0.005	0.252	0.002	0.0164	0.0006	19
0.514	0.005	0.252	0.002	0.0163	0.0006	20
0.513	0.006	0.251	0.002	0.0162	0.0006	21
0.512	0.006	0.251	0.003	0.0162	0.0006	22
0.511	0.006	0.251	0.003	0.0161	0.0006	23
0.511	0.006	0.250	0.003	0.0161	0.0006	24

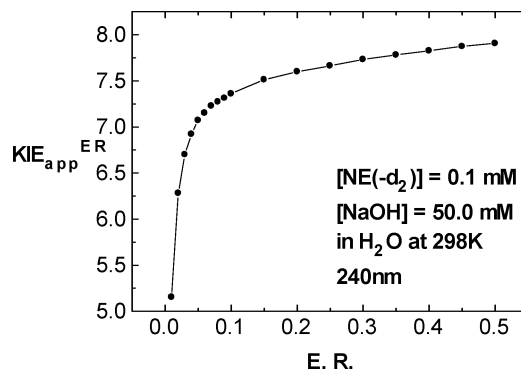
^a [NM] = 0.10 mM, [NaOH] = 20.0 mM, average of 3 sets of 12–20 stopped-flow repetitions. ^b [NE] = 0.10 mM, [NaOH] = 50.0 mM, average of 4 sets of 10–20 stopped-flow repetitions. ^c [2-NP] = 0.10 mM, [NaOH] = 50.0 mM, average of 3 sets of 15–20 stopped-flow repetitions.

involved recording 2000 point absorbance–time (Abs–*t*) profiles over about the first half-lives of the reactions and carrying out a sequential first-order analysis on specific point segments of the Abs–*t* profiles. The procedure also employed least squares linear correlation but in this case 24 different analyses were carried out over different point segments in the profile. The point segments include points 1 to 11, 1 to 21, 1 to 31, 1 to 41, 1 to 51, 1 to 101, 1 to 201, 1 to 301, 1 to 401, 1 to 501, 1 to 601, 1 to 701, 1 to 801, 1 to 901, 1 to 1001, 1 to 1101, 1 to 1201, 1 to 1301, 1 to 1401, 1 to 1501, 1 to 1601, 1 to 1701, 1 to 1801 and 1 to 1901. If a reaction obeys first-order kinetics the values of the rate constants for all of the point segments are expected to be time independent and have the same value. This procedure was described earlier¹⁰ but is repeated here for clarity. A factor that should be taken into account of the data in Table 3 in comparison to that in Fig. 1 is that the former corresponds to 2000 points over the first half-life and the latter to 2000 points over more than 4 half-lives. This difference means that the data segments for Table 3 begin at shorter times than those in Fig. 1.

What is immediately apparent in Table 3 is that in all 3 series of reactions, involving NM, NE and 2-NP as substrates, is that the k_{app} –time profiles begin at relatively high values of k_{app} and decay with time toward steady state values. Although it might be argued that the standard deviations of the short time data in Tables S1 to S3 (ESI†) are relatively high, the mean values of three determinations (Table 3) have a small degree of variance and are certainly significant.

The apparent deuterium kinetic isotope effects (KIE_{app}) for all three nitroalkanes were observed to be E.R. dependent, with a low

value at low conversion and to increase with increasing E.R. This is illustrated in Fig. 2 for the reaction of NE (0.1 mM) with hydroxide ion (50 mM) and for NM and 2-NP in Fig. S1 and S3 (ESI†), respectively. The KIE_{app} –time profiles show a similar trend (Figs. S9 (NM), S10 (NE), and S11 (2-NP)†) but in this case the values are near unity at zero time and approach a constant value at longer times where the reactions reach a steady state.

**Fig. 2** Apparent KIE for the reactions of NE and NE-d₂ as a function of degree of conversion under the conditions shown.

The data discussed in the previous paragraphs clearly rule out a simple 1-step mechanism for the proton transfer reactions between the nitroalkanes and hydroxide ion. Some form of the reversible consecutive mechanism (Mechanism 1 illustrated in Scheme 3) provides a starting point to search for a mechanism that is consistent with the experimental data. The integrated rate law is available for this mechanism.¹⁵

**Scheme 3** The 2-step reversible consecutive mechanism applied to the proton transfer reactions between the nitroalkanes and hydroxide ion in water (Mechanism 1).

In the simplest form of Mechanism 1 (Scheme 3) the intermediate is a preassociation complex in which there are no new covalent bonds formed. Under those circumstances, a steady state would be expected to be reached early in the reaction. However, contrary to the latter, the reactions of the simple nitroalkanes with hydroxide ion in water reported here do not reach a steady state early in the reactions as shown by the data in Table 2. For this reason we believe that Mechanism 1 is unlikely for the proton transfer reactions between the nitroalkanes and hydroxide ion reported here.

A feature of the data in Tables 2 and 3 of great mechanistic significance is that the time dependent k_{app} values for all three substrates decrease from the values at short times toward steady-state values at longer times. The only circumstance that gives rise to this general behavior is when the absorbances monitored, primarily due to the anionic products, also have contributions due to intermediates. For purely product absorbance (Fig. 3a) the time dependent rate constants (k_{inst}) increase from zero to the steady state value for mechanism 1 (Fig. 3b). The most significant point with regard to the presence of an intermediate is that when the apparent absorbance includes both that due to product and a

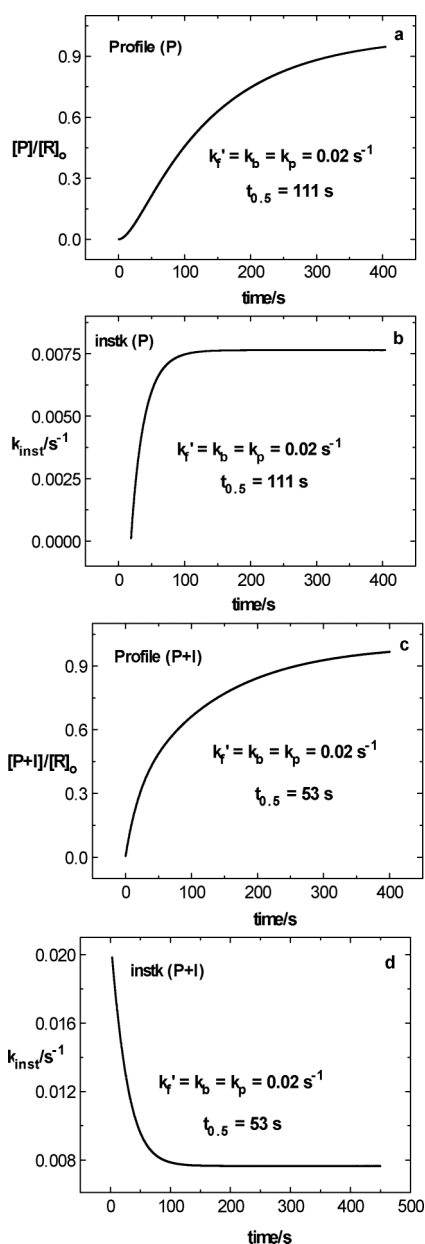


Fig. 3 Simulated concentration–time (a, c) and k_{inst} –time (b, d) profiles for the reversible consecutive mechanism with the rate constants shown. $k_f' = k_r[\text{Excess Reactant}]_0$.

significant contribution from an intermediate (Fig. 3c) the time dependent rate constants decay from an initial value to a steady state value (Fig. 3d). The very different form of the k_{inst} –time profiles for analysis of pure product absorbance (Fig. 3b) and that in the presence of a significant concentration of intermediate (Fig. 3d) provides a very definitive mechanism probe.

Due to the fact that we do not have reliable methods to estimate either the absorbance maximum wavelengths or the extinction coefficients of the intermediates, it is pointless to attempt to fit experimental data to simulated data such as shown in Fig. 3. The simulation (Fig. 3) assumed that the intermediate and product have equal extinction coefficients in the simulated experiment.

The presence of intermediates during the reactions was confirmed by carrying out the diode-array experiments (Fig. 4) near

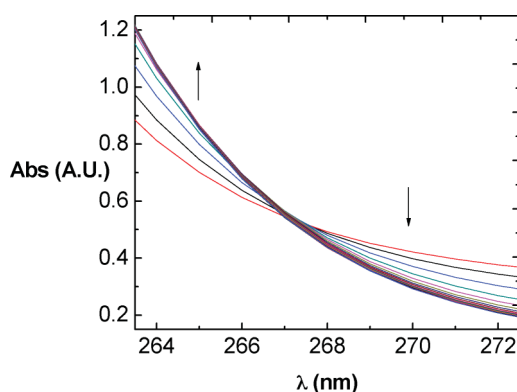


Fig. 4 Diode-array UV absorption spectra of the reaction between NE-d₂ (20.37 mM) and hydroxide ion (100.0 mM) in water at 298 K: start time, 0 s; cycle time, 10 s; total run time, 300 s.

the isosbestic points. There is no true isosbestic point for the absorbance–time curves illustrated in Fig. 4 due to the interference of intermediate absorbance. How the latter can be determined in the presence of absorbance from intermediates is shown in Fig. 6 in the experimental section. The rationale for these experiments was based upon the fact that reactant and product absorbance changes with time are cancelled at the isosbestic point. The absorbance–time data at the isosbestic points in Fig. 5 were obtained during the reaction of (a) NE and (b) NE-d₂ with hydroxide ion in water at 298 K. Absorbance–time curves at isosbestic points are shown in Figs. S5 to S8 (ESI†) for NE, NE-d₂, 2-NP and 2-NP-d₁, respectively.

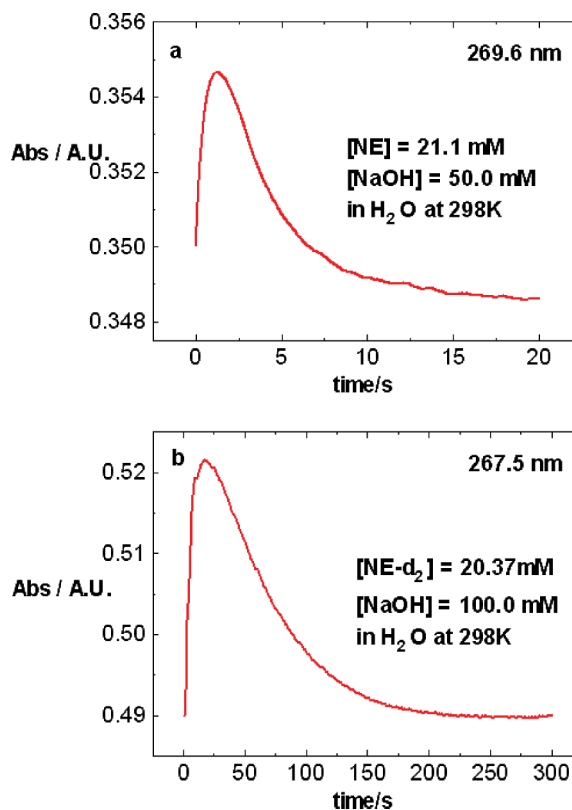
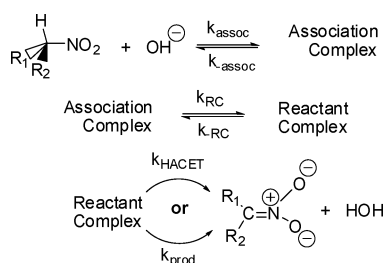


Fig. 5 Abs–time profile at the isosbestic points for the reactions of (a) NE, (b) NE-d₂ with hydroxide ion in water at 298 K.

Simulations show that if the intermediate does not absorb at the isosbestic point, a negative Abs–time profile is observed due to decreases in absorbance of reactant and product accompanying the intermediate formation. This is also the case if the intermediate absorbs with an extinction coefficient less than that of the reactants and product. The fact that positive Abs–time profiles were observed (Fig. 5, S5 to S8†) suggests that the extinction coefficients of the intermediates are greater than that of products and reactants at the isosbestic wavelengths in this study.

It should be pointed out that the Abs–time profiles of the intermediates in Fig. 5 (and Figs. S5 to S8†) were obtained at substrate concentrations much greater than were used in the kinetic experiments. The fact that absorbance due to reactants and products cancel at the isosbestic points made the latter determinations possible. The absorbance due to the intermediates have a lesser effect on the Abs–time profiles under kinetic conditions. The most important effect of intermediate absorbance under kinetic conditions is that illustrated in Fig. 3a as compared to that in Fig. 3c. For the case where only product absorbs (Fig. 3a), there is an evident lag in the onset of product absorbance near zero time while were both product and intermediate to absorb, the absorbance rises sharply from zero time. These facts give rise to a more dramatic effect in the corresponding k_{inst} –time profiles. When only product absorbs, k_{inst} rises from 0 at zero time to a plateau value when steady-state is achieved. When the intermediate also absorbs at the wavelength where product absorbance is monitored, k_{inst} decreases from a relatively large value near zero time to the steady-state plateau value. The latter assumes that the extinction coefficient of the intermediate is sufficiently large to cause an increase in absorbance at the wavelength where product evolution is monitored.

Mechanisms that account for both our kinetic data and for the inverse relationship between the kinetic and thermodynamic acidities of NM, NE and 2-NP are necessary. Mechanism 2 (Scheme 4) involving either an intra-complex electron transfer coupled with hydrogen atom transfer (HACET)¹⁶ or a polar reaction (k_{prod}) as shown in Scheme 4, accounts for the observations. In Mechanism 2 it is assumed that the association complex is in equilibrium (K_{assoc}) with reactants. Simulations of this mechanism showed that to observe the “late” achievement of the steady-state, it requires k_{r} (equal to $k_{\text{RC}}K_{\text{assoc}}$), k_{RC} and k_{HACET} or k_{prod} to be close in magnitude. Our data do not allow us to differentiate between the two possibilities for product forming reactions illustrated in Scheme 4.



Scheme 4 The 3-step reversible consecutive mechanism applied to the reactions between the nitroalkanes and hydroxide ion in water (**Mechanism 2**).

The requirement of rate constants of similar magnitude is demonstrated by the simulated k_{app} –time profile illustrated in Fig. 3. With the three pertinent rate constants equal at a value of 0.02 s^{-1} , nearly three half-lives are required to reach steady-state (Fig. 3d). The inverse relationship between the thermodynamic and kinetic acidity can be explained by either option shown in Mechanism 2. First, the E° values become more negative¹⁷ in the order $\text{NM} > \text{NE} > 2\text{-NP}$ and the values of the equilibrium constants for the formation of the reactant complexes are likely to be in the same order. Taking these factors into account leads to the prediction that the kinetic order for proton transfer to hydroxide ion is $\text{NM} > \text{NE} > 2\text{-NP}$ which is the reverse of the thermodynamic acidity order of the substrates. The second option, direct proton transfer within the reactant complex, is consistent with the observed result simply from the fact that the relative rates of reactions of substrates in a 3-step reaction cannot be predicted from the thermodynamic stabilities of reactants and products.

Some comment is necessary in order to explain how we view the association and reactant complexes to differ. The interactions between OH^- and the nitroalkanes in the former are expected to be relatively weak and the two entities are expected to retain their solvation shells to a large degree. For this reason, the HACET is not expected to be favourable at this stage. We view the formation of the reactant complex to involve extrusion of solvent from the two entities and a change in geometry which allows the concurrent transfer of an electron from hydroxide ion to the nitroalkane and a hydrogen atom from the nitroalkane to hydroxide ion. The changes taking place in going to the reactant complexes would also enhance the favorability of the direct proton transfer.

A question which arises from our work in relation to the previous work on these reactions is: “Why was the complexity in mechanism not observed in the earlier studies?” The work of Bell and Goodall^{3a} was presented in greater detail than other kinetic work on this reaction series. The most important details presented^{3a} which explain why the complexities that we have observed went unnoticed are: (a) the reactions were carried out for only about one half-life and (b) the rates of reaction were followed by a pH-stat, a procedure less reliable than the direct spectrophotometric monitoring of product formation used here.

Experimental

Materials

2-NP- d_1 was prepared by using the literature procedure.^{3a} The other nitroalkanes (NM, NE, 2-NP, NM- d_3 , NE- d_3) were obtained commercially from Sigma-Aldrich and were subjected to an additional purity check by ^1H NMR spectrometry before use. Distilled water was further purified by passing through a Barnsted Nanopure Water System. Concentrated sodium hydroxide solution was commercially available from Fisher Scientific, which had been determined by titration with standard oxalic acid solutions.

Kinetic experiments

Kinetic experiments were carried out using a Hi-Tech SF-61 stopped-flow spectrometer installed in a glove box and kept under

a nitrogen atmosphere. The temperature was controlled at 25 °C using a constant temperature flow system connected directly to the reaction cell in the return pathway to a bath situated outside of the glove box. All stopped flow experiments included recording 10–20 absorbance–time profiles at 240 nm. Each experiment was repeated at least three times. The 2000 point absorbance–time curve data were collected either over 1+ or 5+ half-lives (HL).

Absorbance–time (Abs–*t*) profiles for product evolution were analyzed individually by two different procedures. The first step in both procedures was to convert the Abs–*t* profiles to (1 – E.R.)–time profiles. E.R. denotes extent of reaction, carried out by dividing each absorbance value by the maximum absorbance value obtained in the long-time (>10 HL) kinetic runs, when the reaction goes to completion, such as the profiles shown in Fig. 1. This procedure gave (1 – E.R.)–time profiles that decayed from (1 – E.R.) = 1 for either 1 or 5 HL depending on which analysis procedure was used. For pseudo first-order kinetic analysis the (1 – E.R.)–time profiles were converted to ln(1 – E.R.)–time profiles. For further processing, the individual 5 HL (1 – E.R.)–time profiles were first averaged to give the average profiles.

The first kinetic procedure used was simply least squares linear correlation of the ln(1 – E.R.)–time profiles to give the apparent pseudo first-order rate constants over either 1 or 5 HL. These values are recorded in the Results section. The second kinetic procedure, the modified pseudo first-order analysis, has been described in detail in the former section. The second procedure involved recording the Abs–time profiles over slightly more than the 1st HL followed by the sequential 24 linear correlations described in the Results section.

Determination of isosbestic points

The diode-array kinetic experiments were carried out near the apparent isosbestic points using an Agilent 8453 UV-vis. spectrophotometer. The start time and cycle time were set equal to 0 s and 1 s, respectively. The total run time was dependent upon how long the reaction takes to reach completion. The resulting Abs–*t* profiles, recorded at an interval of 1 s, were first converted to ΔAbs–time profiles by subtracting the initial value from each absorbance value.

It was pointed out earlier that true isosbestic points were not observed due to the contributions of absorbance of the intermediates. This is very obvious for the reactions of NE–d₂ (Fig. 4) and 2-NP–d₁ (Fig. S8, ESI†) in which cases the lifetime of the intermediates appears to be the longest observed. The latter is based upon the fact that the absorbance observed due to the intermediate is substantially greater than all other cases studied (see Fig. S5, S7, ESI†). The wavelength judged to be most close to the true isosbestic point was selected based upon the comparison of the ΔAbs–time profiles as shown in Fig. 6. Although the absolute absorbance values are not known, due to inherent instrumental error, the ΔAbs values are expected to be reliable and have been verified by multiple determinations. The ΔAbs–time profile judged to be most significant is that with the long-time value approaching zero since the concentration of intermediate is expected to approach zero as the reaction goes to completion.

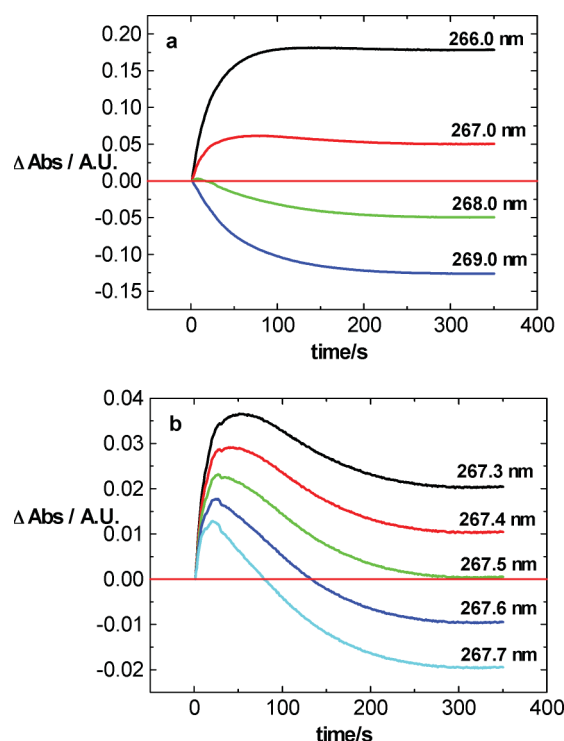


Fig. 6 ΔAbs–time profiles for the reaction of NE–d₂ (20.37 mM) with hydroxide ion (50.0 mM) in water at 298 K near the isosbestic point, 267.5 nm (a: from 266.0 nm to 269.0 nm with an increment of 1.0 nm; b: from 267.3 nm to 267.7 nm with an increment of 0.1 nm). ΔAbs = Abs_{*t*} – Abs₀.

Conclusions

The proton transfer reactions of NM, NE and 2-NP with hydroxide ion in water take place by a complex mechanism. This conclusion is supported by conventional 1st-order analysis as well as by a sequential 1st-order analysis designed to show changes in the apparent pseudo-first-order rate constant if they exist. For all three reactions the *k*_{app} were observed to be relatively large at short times and decrease toward steady-state values later in the reaction. Absorbance–time profiles at isosbestic points show the presence of intermediates which absorb at these wavelengths. The absorbances due to intermediates are most persistent for NE–d₂ (compare the time scales in Figs. S5 and S6†) and 2-NP–d₁ (compare the time scales in Fig. S7 and S8†) in which the acidic protons are replaced by deuterons. The latter indicates that the deuterium kinetic isotope effects are not associated with the formation of the intermediates. This is also illustrated by the fact that the KIE are E.R. dependent approaching unity near zero time and increasing toward a plateau value as steady-state is achieved. A reversible consecutive mechanism is proposed with two possible product forming steps involving either a polar proton transfer or an intra-complex H Atom Coupled Electron Transfer from a “Reactant Complex”.

Acknowledgements

This work was supported by a grant (ARRA: CHE-0923654) from the National Science Foundation. This support is gratefully acknowledged.

References

- 1 (a) S. H. Maron and V. K. La Mer, *J. Am. Chem. Soc.*, 1938, **60**, 2588; (b) D. Turnbull and S. H. Maron, *J. Am. Chem. Soc.*, 1943, **65**, 212; (c) G. W. Wheland and J. Farr, *J. Am. Chem. Soc.*, 1943, **65**, 1433; (d) R. G. Pearson and R. L. Dillon, *J. Am. Chem. Soc.*, 1953, **75**, 2439.
- 2 A. J. Kresge, *Can. J. Chem.*, 1975, **52**, 1897.
- 3 (a) R. P. Bell and D. M. Goodall, *Proc. R. Soc. London, Ser. A*, 1966, **294**, 273; (b) F. G. Bordwell, W. Boyle, Jr., J. A. Hautala and K. C. Yee, *J. Am. Chem. Soc.*, 1969, **91**, 4002; (c) P. W. Fukuyama, K. Flanagan, F. T. Williams, Jr., L. Frainier, S. A. Miller and H. Shechter, *J. Am. Chem. Soc.*, 1970, **92**, 4689; (d) A. J. Kresge, *J. Am. Chem. Soc.*, 1970, **92**, 3210; (e) F. G. Bordwell and W. J. Boyle Jr., *J. Am. Chem. Soc.*, 1971, **93**, 512; (f) A. J. Kresge, H.-L. Chen, Y. Chiang, E. Murrill, M. A. Payne and D. S. Sagatys, *J. Am. Chem. Soc.*, 1971, **93**, 413; (g) F. G. Bordwell and W. J. Boyle Jr., *J. Am. Chem. Soc.*, 1972, **94**, 3907; (h) R. A. Marcus, *J. Am. Chem. Soc.*, 1969, **91**, 7224; (i) N. Agmon, *J. Am. Chem. Soc.*, 1980, **102**, 2164; (j) W. J. Albery, C. F. Bernasconi and A. J. Kresge, *J. Phys. Org. Chem.*, 1988, **1**, 29.
- 4 J. R. Keefe, J. Morey, C. A. Palmer and J. C. Lee, *J. Am. Chem. Soc.*, 1979, **101**, 1295.
- 5 (a) J. R. Gandler and C. F. Bernasconi, *J. Am. Chem. Soc.*, 1992, **114**, 631; (b) C. F. Bernasconi, D. Wiersema and M. W. Stronach, *J. Org. Chem.*, 1993, **58**, 217; (c) C. F. Bernasconi and J.-X. Ni, *J. Org. Chem.*, 1994, **59**, 4910; (d) C. F. Bernasconi, M. Panda and M. W. Stronach, *J. Am. Chem. Soc.*, 1995, **117**, 9206; (e) C. F. Bernasconi and R. L. Montañez, *J. Org. Chem.*, 1997, **62**, 8162; (f) C. F. Bernasconi and K. W. Kittredge, *J. Org. Chem.*, 1998, **63**, 1994; (g) C. F. Bernasconi, M. Ali and J. C. Gunter, *J. Am. Chem. Soc.*, 2003, **125**, 151; (h) C. F. Bernasconi, M. Pérez-Lorenzo and S. D. Brown, *J. Org. Chem.*, 2007, **72**, 4416.
- 6 (a) C. F. Bernasconi, P. J. Wenzel, J. R. Keefe and S. Gronert, *J. Am. Chem. Soc.*, 1997, **119**, 4008; (b) H. Yamataka, Mustanir and M. Mishima, *J. Am. Chem. Soc.*, 1999, **121**, 10223; (c) C. F. Bernasconi and P. J. Wenzel, *J. Am. Chem. Soc.*, 2001, **123**, 2430; (d) C. F. Bernasconi and P. J. Wenzel, *J. Org. Chem.*, 2003, **68**, 6870; (e) J. R. Keefe, S. Gronert, M. E. Colvin and N. L. Tran, *J. Am. Chem. Soc.*, 2003, **125**, 11730; (f) H. Yamataka and S. C. Ammal, *ARKIVOC*, 2003, 59; (g) M. Sato, Y. Kitamura, N. Yoshimura and H. Yamataka, *J. Org. Chem.*, 2009, **74**, 1268.
- 7 F. G. Bordwell and W. J. Boyle, Jr., *J. Am. Chem. Soc.*, 1975, **97**, 3447.
- 8 C. F. Bernasconi, D. A. V. Kliner, A. S. Mullin and J. X. Ni, *J. Org. Chem.*, 1988, **53**, 3342.
- 9 J. C. Wilson, I. Kallsson and W. H. Saunders Jr., *J. Am. Chem. Soc.*, 1980, **102**, 4780.
- 10 V. D. Parker, Z. Li, K. L. Handoo, W. Hao and J.-P. Cheng, *J. Org. Chem.*, 2011, **76**, 1250.
- 11 K. L. Servis, *J. Am. Chem. Soc.*, 1965, **87**, 5495; K. L. Servis, *J. Am. Chem. Soc.*, 1967, **89**, 1508.
- 12 (a) Y. Zhao, Y. Lu and V. D. Parker, *J. Am. Chem. Soc.*, 2001, **123**, 1579; (b) V. D. Parker, *Pure Appl. Chem.*, 2005, **77**, 1823.
- 13 F. T. Williams, Jr., P. W. K. Flanagan, W. J. Taylor and H. Shechter, *J. Org. Chem.*, 1965, **30**, 2674.
- 14 V. D. Parker, *J. Phys. Org. Chem.*, 2006, **19**, 714. Reviewers sometimes object to referring to $\ln(1 - ER)$ vs. time as the conventional 1st-order relationship. This is the general relationship which arises from the integration of the 1-step mechanism where ER refers to $[\text{product}]/[\text{reactant}]_0$ when $[\text{product}]$ is monitored and to $(1 - [\text{reactant}]/[\text{reactant}]_0)$ when $[\text{reactant}]$ is monitored.
- 15 H. S. Johnston, *Gas Phase Reaction Rate Theory*, Ronald Press, Berkeley, Appendix, p. 439. A pair of brackets was omitted in third equation in (A-3) on p. 439.
- 16 It seems reasonable to suggest that electron tunneling will allow thermodynamically unfavorable inter-complex electron transfer to take place at rates greatly exceeding estimations based upon E° differences.
- 17 D. H. Evans and A. G. Gilieinski, *J. Phys. Chem.*, 1992, **96**, 2528.